Measurements and CFD simulations of flow and dispersion in urban geometries

Valeria Garbero* and Pietro Salizzoni

Dipartimento di Ingegneria Aeronautica e Spaziale,
Politecnico di Torino, Corso Einaudi, 24 Torino, Italia
E-mail: valeria.garbero@polito.it
E-mail: pietro.salizzoni@polito.it
*Corresponding author

Lionel Soulhac and Patrick Mejean

Laboratoire de Mécanique des Fluides et d'Acoustique,
UMR CNRS 5509,
University of Lyon, Ecole Centrale de Lyon, INSA Lyon,
Université Claud Bernard Lyon I,
36, Avenue Guy de Collongue, 69134 Ecully, France
E-mail: lionel.soulhac@ec-lyon.fr
E-mail: patrick.mejan@ec-lyon.fr

Abstract: Dispersion in urban areas is determined by transport and mixing processes within the street network and ventilation into the external atmosphere. In order to improve the understanding of the exchange mechanisms within the urban canopy, wind tunnel and numerical investigations have been performed on two idealised typical urban configurations, the street intersection and the square. The numerical simulations were compared to the experimental values, in order to evaluate the reliability of the numerical approach in simulating local flow patterns and study the influence of the geometrical layout on mass and momentum exchange mechanisms.

Keywords: atmospheric dispersion; urban intersection; wind-tunnel experiment; numerical simulation.

Reference to this paper should be made as follows: Garbero, V., Salizzoni, P., Soulhac, L. and Mejean, P. (xxxx) 'Measurements and CFD simulations of flow and dispersion in urban geometries', *Int. J. Environment and Pollution*, Vol. x, pp.xxx–xxx.

Biographical notes: Valeria Garbero received her PhD in Environmental Fluid Mechanics from the Politecnico of Turin and from the Ecole Centrale of Lyon. Her research studies concern the pollutant dispersion in urban areas, which are conducted through wind tunnel experiments and numerical simulations.

Pietro Salizzoni received his PhD in Environmental Fluid Mechanics from the Politecnico of Turin and from the Ecole Centrale of Lyon. His research activities deal with flow over rough walls, mass and momentum exchange in cavity flows and smoke propagation in tunnels.

Lionel Soulhac is Maître des Conferences at the Ecole Centrale de Lyon. His research activity mainly concerns pollutant dispersion modelling in urban areas and inverse modelling for risk evaluation in industrial sites.

Patrick Mejean is a research engineer at the Ecole Centrale de Lyon. His research activity mainly focuses on the experimental studies of the pollutant dispersion in complex areas.

1 Introduction

Squares and street intersections play an important role in pollutant dispersion, as they represent regions of pollutant exchanges between different streets. Different studies focused on the influence of the intersection geometry and external wind direction on flow dynamics and dispersion mechanisms in urban configurations (Dabbert et al., 1995; Robins et al., 2002; Soulhac et al., 2001).

This paper contains both wind tunnel experiments and numerical simulations of flow and dispersion in typical urban configurations, such as a square and a street intersection. The street intersection consisted of two crossing orthogonal streets, whose widths were varied to obtain three different configurations.

The numerical and wind tunnel set up are described in Section 2. In Section 3.1 the flow field is analysed and the experimental data are compared with numerical simulations in order to evaluate CFD as a tool for simulating flow in urban geometries. In Section 3.2 the concentration measurements are examined in order to highlight the effect of the geometrical layout on the pollutant dispersion. In Section 4, the results are discussed and the conclusions concerning the exchange mechanisms at street intersections are drawn.

2 Experimental and numerical set up

The wind-tunnel investigations were conducted in a recirculating wind tunnel at the LMFA, Ecole Centrale de Lyon, whose test section is 14 m long × 3.7 m wide × 2.5 m high. A neutrally stratified boundary layer of 800 mm height was generated by combining the Irwin spires (Irwin, 1981) with roughness elements placed on the floor. In order to avoid perturbations of the flow due to roughness changes (Belcher et al., 2003), the studied configurations were embedded in an array of identical obstacles simulating an idealised urban neighbourhood, as shown in Figure 1(a). The obstacles were aligned and measured $H \times 5H \times 5H$, where H was 50 mm, representing simplified urban blocks of 20 m height at a scale factor of 1 : 400. The external flow simulated a neutral urban atmospheric boundary layer in equilibrium conditions; the external free stream velocity U_∞ was 5 m/s. The mean velocity profile was fitted in the inertial layer to the typical logarithmic law:

$$U(z) = \frac{u_*}{k} \ln\left(\frac{z-d}{z_0}\right) \tag{1}$$

where the friction velocity was $u_* = 0.27$ m/s, the roughness height $z_0 = 0.5$ mm and the displacement height $d = 50$ mm. The three different *street intersections* were obtained by

varying the spacing between the obstacles, as shown in Figure 1(b)–(d): $S_x = S_y = H$ for configuration 1, $S_x = 2H$ and $S_y = H$ for configuration 2, $S_x = H$ and $S_y = 2H$ for configuration 3. The *square* measured $L = 5H$ in width and length and the width of the street was $S_x = S_y = H$, as shown in Figure 1(e). In the present study we took into account only the case of a wind direction parallel to the x-axis, as indicated by the arrow in Figure 1(a). A passive tracer was released from a point source, which has been placed within the array at height $z = H/2$ at the upwind intersection.

Flow field investigations were performed by means of Laser Doppler Anemometry, while concentration profiles were measured by the Flame Ionisation Detector.

Figure 1 Wind-tunnel set up: (a) the overall array; (b) intersection, $S_x = S_y = H$; (c) intersection, $S_x = 2H$ and $S_y = H$; (d) configuration 3, $S_x = H$ and $S_y = 2H$ and (e) square, $L = 5H$

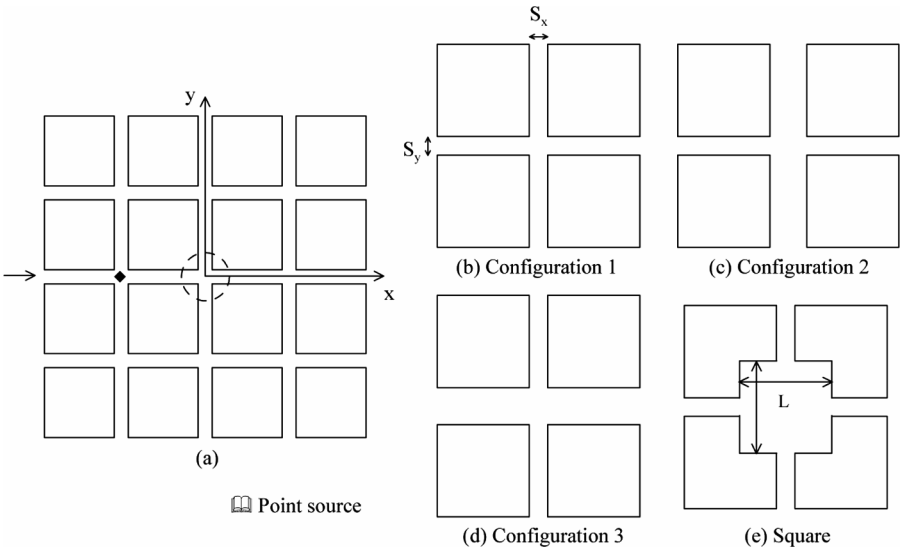

The numerical simulations were performed by means of the commercial code FLUENT and a standard k–ε turbulence model was implemented. In order to limit the computing time, the numerical domain consisted of a single intersection; in order to simulate the whole obstacle array periodical conditions were set on the inlet and the outlet and conditions of symmetry were set on the top and on the lateral boundaries. Such an approach could not be applied to the case of the square, since the domain is not periodic. In this case the overall array was simulated. In the numerical simulations, the roughness length of the obstacle wall was adjusted in order to achieve the best agreement between the simulated external velocity profile and the experimental one.

3 Results

3.1 Flow field

Experimental and numerical investigations have been performed in order to study the flow dynamics within the urban configurations.

As a first step, numerical data have been compared with the experimental measurements in order to evaluate the CFD as tool for simulating the flow in urban geometries. In Figure 2 numerical and experimental transversal profiles of the longitudinal mean velocity U are presented for configurations 1 and 3. The profiles were traced along the y-axis, at $z/H = 0.5$ and $x = 0$.[1] The numerical results show good agreement with the experimental measurements, thus supporting the use of the numerical approach to investigate the flow dynamics in complex geometries.

Figure 2 Mean velocity transversal profiles at $z = H/2$: (a) configuration 1 and (b) configuration 3. Dashed lines indicate the interface between the intersection and the crossing street

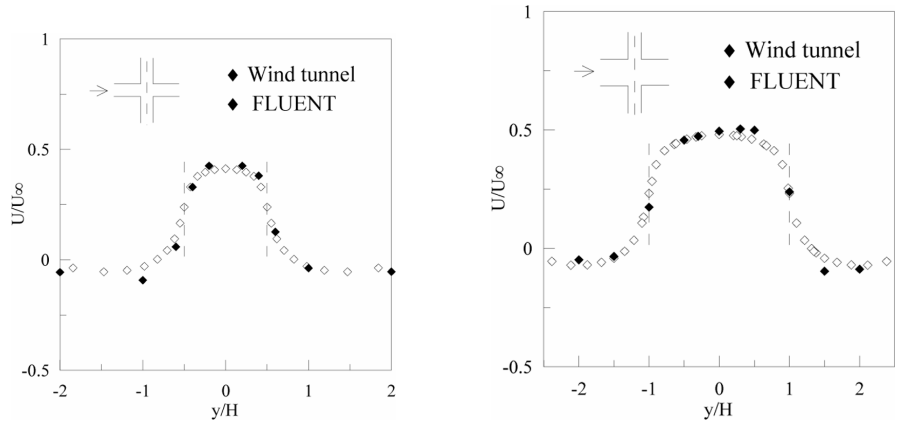

Numerical simulations have then been employed to visualise the main features of the flow field in the three different configurations. Figure 3 shows the velocity field on the horizontal plane at height $z = H/2$ and the 3-d streamlines (grey lines) crossing the rake A and B that suggest the mean flow characteristics. The flow within the intersection is imposed by the direction of the external wind and drives the vortical motion within the street $n°$ 2. A mean flow directed from the intersection towards the street is detected, while no streamlines coming from the street $n°$ 2 crosses the street $n°$ 1. The topology of the streamlines close to the interface between the intersection and the street $n°$ 2, whose understanding is essential to envisage the pollutant exchange mechanisms, is quite complex and depends on S_x, the size of the interface. It is worth noting that the configurations which are characterised by the same spacing of the street $n°$ 2, $S_x = H$– Figure 3(a) and (c) – show similar flow dynamics. In this case, the vertical axis vortex taking place within the street $n°$ 2 weakly interacts with the flow in the street $n°$ 1 that appears to be channelled. An analogy may be drawn with the flow regime over a sufficiently packed obstacles array, which is usually referred to as the skimming flow regime (Oke, 1988). Conversely, for a twice spaced interface, i.e., $S_x = 2H$, the topology of the flow within the street intersection is significantly different. The recirculation cell with vertical axis occurring close to the interface is confined to the upwind corner and several streamlines are directed from the street $n°$ 1 towards the street $n°$ 2. The higher complexity of the flow dynamics is similar to that occurring in a wake interference flow (Oke, 1988).

Figure 3 (a) Positioning of rakes *A* and *B* within the street intersections; (b) mean velocity field at the street intersections in configuration 1; (c) configuration 2 and (d) configuration 3. Streamlines are represented with grey lines, see text for details

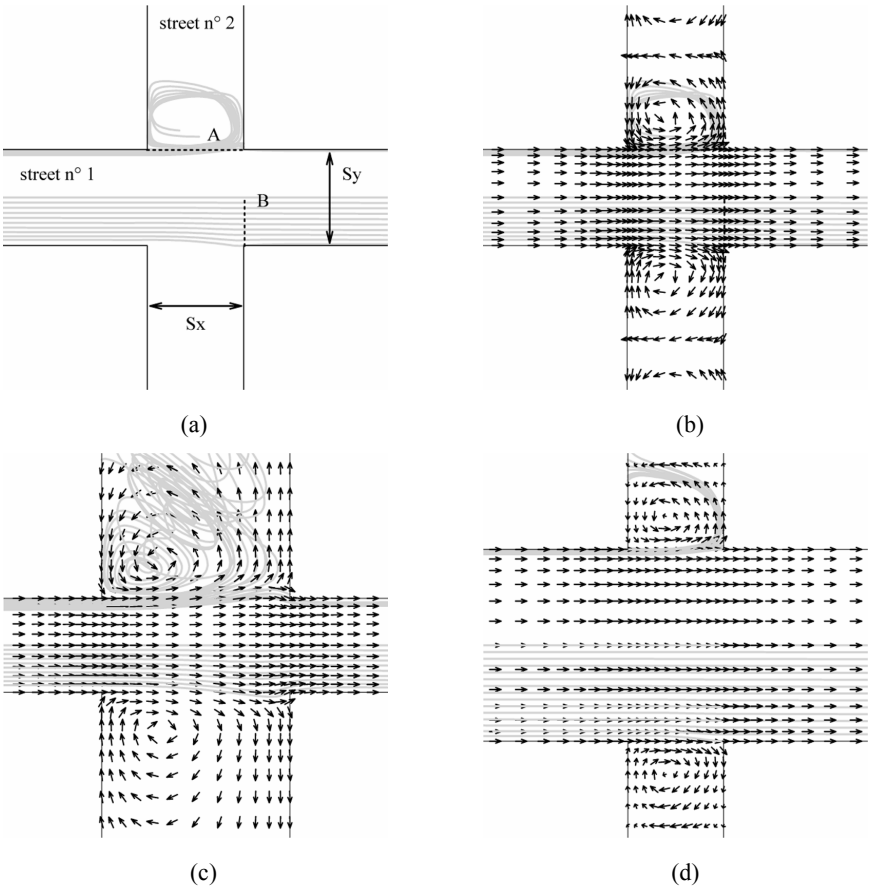

A further analysis concerned another usual urban configuration, the square. The numerical results were compared with the measured values: Figure 4 shows the transversal profiles of the mean velocity component U performed at $z = H/2$ in the centre of the square ($x = 0$), upwind ($x = -2H$) and downwind ($x = 2H$). Also in this case, numerical and experimental results agree well.

A more accurate analysis of the flow dynamics within the square could be performed by means of numerical simulations. In Figure 5 horizontal and vertical sections of the velocity field are displayed; a contour line identifying the condition $U = 0$ is plotted, to say when the x-axis component of the mean velocity changes direction and a recirculating motion takes place. The flow coming from the upstream street acts as driving flow together with the external flow and generates the recirculating turbulent structures occurring at the upwind corners of the square. The driving effect of the flow coming from the street *n*° 1 is evident in Figure 5(a), where the presence of two

counter-rotating vortices with vertical axes in the upwind corners is shown. In order to enlighten the role of the external flow, longitudinal vertical sections of the mean longitudinal velocity calculated at $y = H/2$ and at $y = -H$ are shown in Figure 5(b)–(c). The contour line matching the condition $U = 0$ indicates that two co-rotating vortices of the horizontal axis originate in the upwind and downwind corners, driven by the external wind. The dimension and the structure of the recirculating region vary with the position within the square. At the interface between the square and the street $n°$ 2, the velocity field is not decoupled as in configuration 1, even if the street aspect ratio is the same, i.e. $S_x/H = 1$. A mean flow component is directed towards the street $n°$ 2 and interacts with the recirculating motion in the street, originating a helicoidal movement within it.

Figure 4 Mean velocity transversal profiles within a square: (a) $x = -2H$; (b) $x = 0$ and (c) $x = 2H$

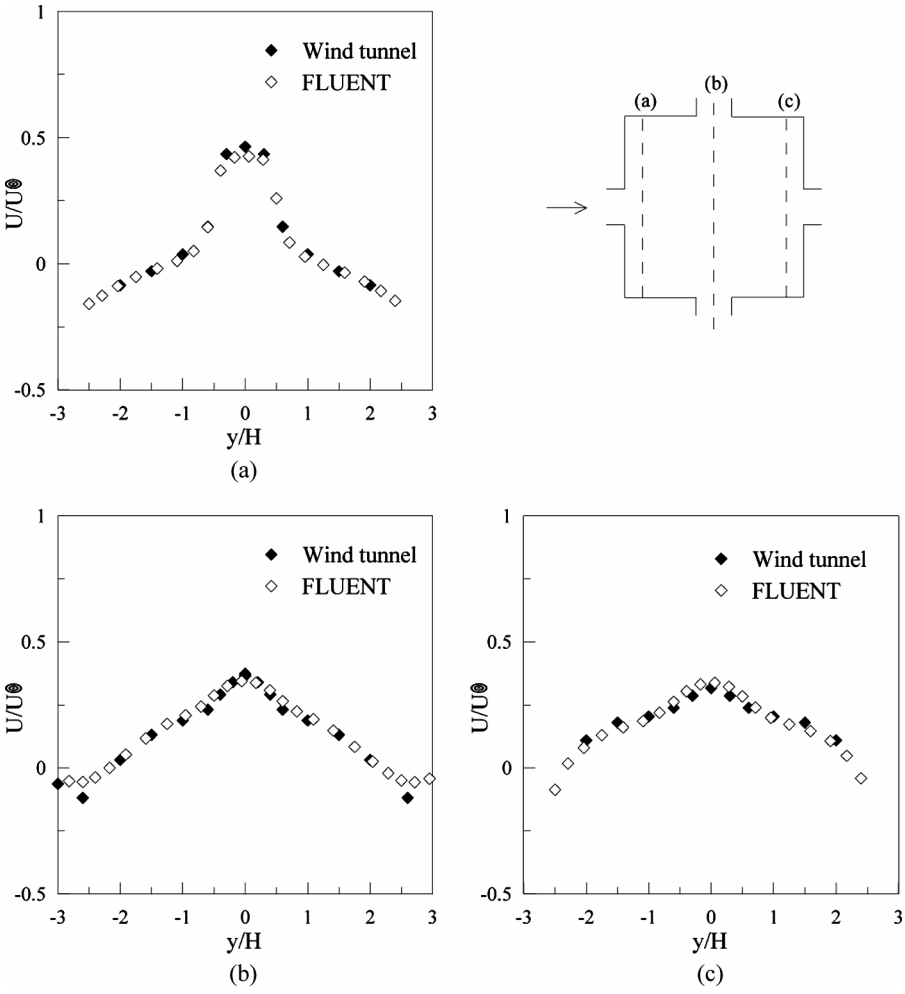

Figure 5 Numerical velocity vector field on horizontal and vertical sections: (a) $z = H/2$; (b) $y = 2H$ and (c) $y = -H$. The continuous line identifies the condition $U = 0$ (see online version for colours)

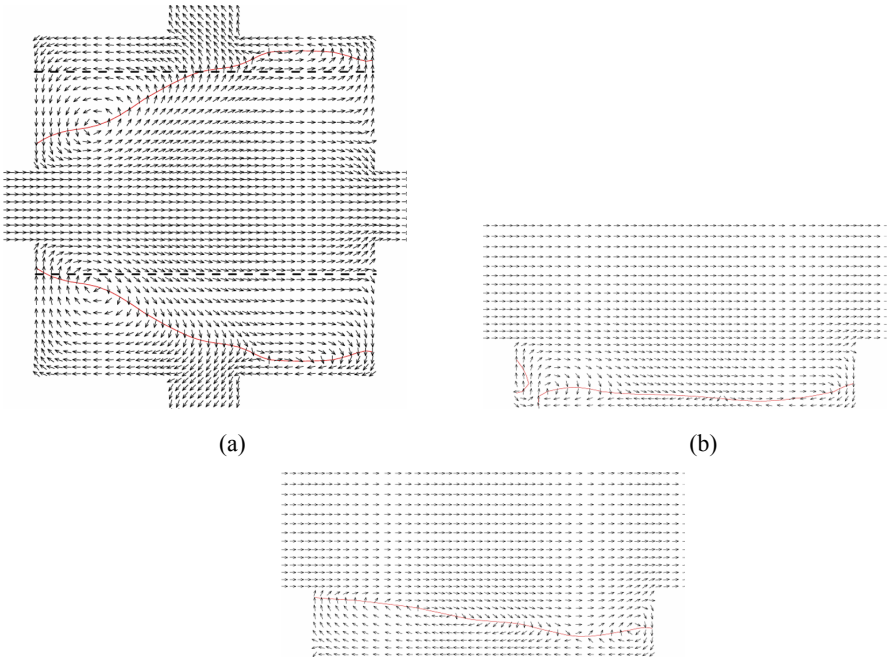

(a) (b)

(c)

3.2 Passive scalar dispersion

The influence of the intersection layout on the pollutant transport and the exchange phenomena have been investigated experimentally; the data have been analysed and interpreted in the light of what could be inferred about the flow dynamics. The mean concentrations are presented in a standard dimensionless form:

$$K = \frac{CUHL}{Q} \tag{2}$$

where C is the measured mean concentration, Q is source emission rate, U the velocity at the roof level, H the height and L the length of the obstacles. In Figure 6(a)–(c), the transversal profiles of the mean concentration performed at height $z = H/2$ are plotted for the different street intersections and are fitted to a Gaussian profile, as suggested by numerous authors (Macdonald et al., 1998; Gailis and Hill, 2006):

$$K = K_{\max} \exp\left[-\frac{y^2}{2\sigma_y^2}\right]. \tag{3}$$

Figure 6 Experimental mean concentration transversal profiles and Gaussian fit (grey lines) at street intersection: (a) configuration 1; (b) configuration 3; (c) configuration 2. (d) σ_y values as function of the street aspect ratio for the different street intersections. Dot lines indicate the interface between the intersection and the street *n*° 2

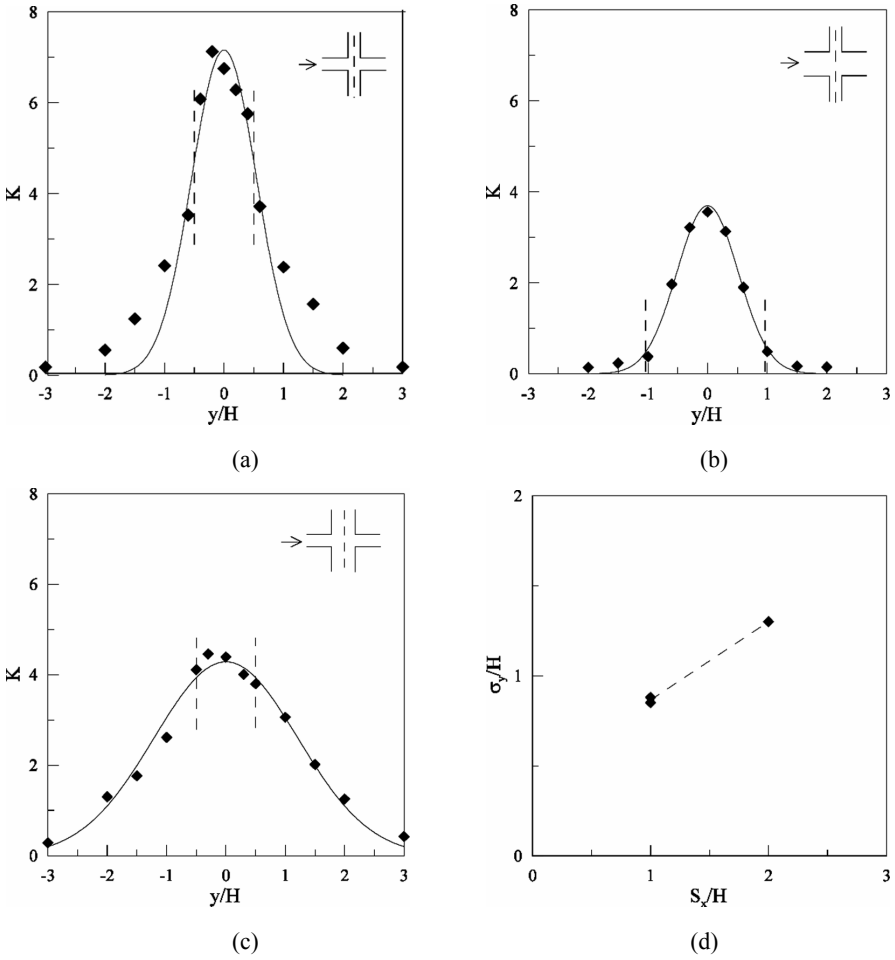

The Gaussian fit describes quite well the concentration distribution for the street intersection in the case $S_x/H = 2$ (Figure 6(c)). Conversely, when $S_x/H = 1$ the Gaussian distribution fits the measured concentrations within the intersection but not in the adjacent streets; this is particularly evident in the configuration 1, as shown in Figure 6(a). The standard deviation σ_y quantifies the horizontal spreading of the plume and is controlled by the street spacing S_x/H, the geometrical parameter characterising the exchange surface between the intersection and the street *n*° 2 (Figure 6(d)). The different behaviour of the plume spreading is coherent with the different flow regimes identified in the previous paragraph. For $S_x/H = 1$ a skimming flow regime takes place; the flow dynamics in the street *n*° 1 is somehow decoupled from the flow in the adjacent street and the channelling effect along the *x*-axis limits the pollutant exchange and, thus, the plume spreading. For $S_x/H = 2$, the flow dynamics is similar to that occurring in a wake-interference regime; the higher interaction of the flow among the two streets

induces enhanced mixing process, that result in a smoothed pollutant concentration distribution.

In case of the square, the transversal profiles of the mean concentration performed within the square ($x = -2H$, $x = 0$ and $x = 2H$) at $z = H/2$ are displayed in Figure 7.

Figure 7 Experimental mean concentration transversal profiles and Gaussian fit (grey lines) at $z = H/2$ within the square: (a) $x = -2H$, (a) $x = 0$ and (a) $x = 2H$

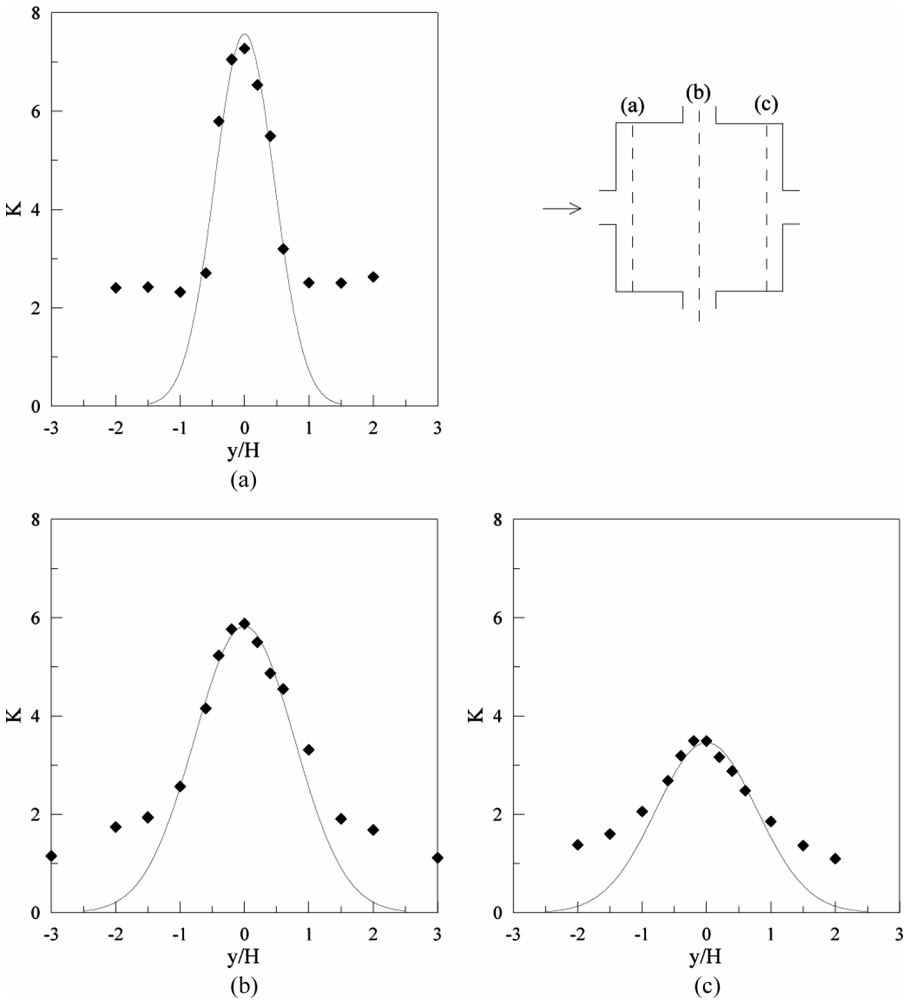

Also in this case, a qualitative comparison with a Gaussian profile is presented. Except for the central region, i.e., $-H/2 < y < H/2$, the concentration distributions do not follow the Gaussian fit. The homogenisation of the concentration values on the sides clearly indicates that intense mixing processes are present, taking place within the recirculating cells in the upwind and downwind corners. Two mechanisms of pollutant transfer can then be identified within the square: the streamwise transport due to the channelled flow coming from the upwind street and the turbulent mixing that rapidly diffuses the pollutants at the side of the square and makes homogeneous the concentration field due to vortical structures.

4 Conclusions

Flow and dispersion in urban geometries have been studied by means of experimental and numerical methods. The numerical simulations agree well with the experimental data, showing the potentiality of a k–ε model to describe the flow in urban configurations.

The flow pattern and the plume spreading are strongly affected by the geometrical layout. In the case of the street intersections, the exchange processes depends on the size of the exchange surface between the intersection and the crossing street and the key parameter is then S_x/H. For $S_x/H = 1$ a skimming flow regime occurs and the channelling effect limits the pollutant exchange; for $S_x/H = 2$ a wake interference flow regime takes place and the concentration distribution shows a higher lateral spreading of the pollutant plume. In the case of the square, more complicated mass and momentum exchange mechanisms occur, due to the interaction between the channelled flow in the centre and the recirculating motions taking place at the sides.

References

Belcher, S.E., Jerram, N. and Hunt, J.C.R. (2003) 'Adjustment of a turbulent boundary layer to a canopy of roughness elements', *J. Fluid Mech.*, Vol. 488, pp.369–398.

Dabbert, W., Hoydysh, W., Schoring, M., Yang, F. and Holynskyi, O. (1995) 'Dispersion modelling at urban intersection', *Sci. Total Env.*, Vol. 169, pp.93–102.

Gailis, R.M. and Hill, A. (2006) 'A wind-tunnel simulation of plume dispersion within a large array of obstacles', *Boundary Layer Meteorology*, Vol. 119, pp.289–338.

Irwin, H.P.A.H. (1981) 'The design of spires for wind simulation', *J. Wind Eng. Ind. Aerodyn*, Vol. 7, pp.361–366.

Macdonald, R.W., Griffiths, R.F. and Hall, D.J. (1998) 'A comparison of results from scaled field and wind tunnel modelling of dispersion in arrays of obstacles', *Atmospheric Environment*, Vol. 32, pp.3845–3862.

Oke, T.R. (1988) 'Street design and urban canopy layer climate', *Energy and Buildings*, Vol. 11, pp.103–113.

Robins, A., Savory, E., Scaperdas, A. and Grigoriadis, D. (2002) 'Spatial variability and source-receptor relations at a street intersection', *Water Air Soil Pollut.: Focus*, Vol. 2, pp.381–393.

Soulhac, L., Mejean, P. and Perkins, R.J. (2001) 'Modelling the transport and dispersion of pollutants in street canyons', *Int. J. Environment and Pollution*, Vol. 16, pp.404–413.

Note

[1]The origin of the reference system is set at the centre of the intersection, as shown in Figure 1.